Title

Anterior Cingulate Cortex Ablation Disrupts Affective Vigor and Vigilance.

Journal

Journal of Neuroscience, 41(38)

ISSN

0270-6474

Authors

Bliss-Moreau, Eliza
Santistevan, Anthony C
Bennett, Jeffrey
et al.

Publication Date

2021-09-22

DOI

10.1523/jneurosci.0673-21.2021

Peer reviewed

Behavioral/Cognitive

Anterior Cingulate Cortex Ablation Disrupts Affective Vigor and Vigilance

Eliza Bliss-Moreau,[1,2] Anthony C. Santistevan,[1,2] Jeffrey Bennett,[1,2,3,4] Gilda Moadab,[1,2] and David G. Amaral[3,4]

[1]Department of Psychology, University of California, Davis, Davis, California 95616, [2]California National Primate Research Center, University of California, Davis, Davis, California 95616, [3]Department of Psychiatry and Behavioral Sciences, School of Medicine, University of California, Davis, Davis, California 95817, and [4]The MIND Institute, School of Medicine, University of California, Davis, Davis, California 95817

Despite many observations of anterior cingulate cortex (ACC) activity related to cognition and affect in humans and nonhuman animals, little is known about the causal role of the ACC in psychological processes. Here, we investigate the causal role of the ACC in affective responding to threat in rhesus monkeys (*Macaca mulatta*), a species with an ACC largely homologous to humans in structure and connectivity. Male adult monkeys received bilateral ibotenate axon-sparing lesions to the ACC (sulcus and gyrus of areas 24, 32, and 25) and were tested in two classic tasks of monkey threat processing: the human intruder and object responsiveness tasks. Monkeys with ACC lesions did not significantly differ from controls in their overall mean reactivity toward threatening or novel stimuli. However, while control monkeys maintained their reactivity across test days, monkeys with ACC lesions reduced their reactivity toward stimuli as days advanced. Critically, this attenuated reactivity was found even when the stimuli presented each day were novel, suggesting that ACC lesions did not simply cause accelerated adaptation to stimuli as they became less novel over repeated presentations. Rather, these results imply that the primate ACC is necessary for maintaining appropriate affective responses toward potentially harmful and/or novel stimuli. These findings therefore have implications for mood disorders in which responding to threat and novelty is disrupted.

Key words: **ACC; affective reactivity; anterior cingulate cortex; threat**

Significance Statement

Decades of research in humans and nonhuman animals have investigated the role of the anterior cingulate cortex in a huge number and variety of psychological processes spanning cognition and affect, as well as in psychological and neurologic diseases. The structure is broadly implicated in psychological processes and mental and neurologic health, yet its causal role in these processes has largely gone untested, particularly in primates. Here we demonstrate that when anterior cingulate cortex is completely eliminated, rhesus monkeys are initially responsive to threats, but these responses attenuate rather than persist, resembling a pattern of behavior commonly seen in patients diagnosed with mood disorders.

Introduction

So many psychological processes correlate with activity and structure of the anterior cingulate cortex (ACC) that hypotheses about its function have been likened to Rorschach blots—reflecting researchers' own biases more than the actual computations of the ACC (Ebitz and Hayden, 2016). Consistent with its broad involvement in psychological phenomena (for review, see Bartra et al., 2013; Lindquist et al., 2012; Seeley, 2019), dysfunction of the ACC is observed across many psychiatric conditions, particularly in those with socioaffective clinical indications including anxiety, depression, and bipolar disorder (Mulders et al., 2015; Perry et al., 2019; Roberts, 2020). Its involvement in so many psychological functions and dysfunctions make it an ongoing target of study relative to understanding mechanisms of mental health and to the development of treatment and interventions for disorders (Rudebeck et al., 2019).

One of the central roles of the ACC appears to be in affect-related processes (for review, see Rolls, 2019) in support of cognitive processes like decision-making and attention. These functions are thought to be supported by the ACC itself, and its function in the networks in which it is situated (Pandya et al., 1981; Barbas and Pandya, 1989; Stefanacci and Amaral, 2002; Vogt et al., 2005; for review, see Heilbronner and Hayden, 2016).

Received Mar. 22, 2021; revised July 19, 2021; accepted July 24, 2021.

Author contributions: E.B.-M., J.B., G.M., and D.G.A. designed research; E.B.-M., A.C.S., J.B., G.M., and D.G.A. performed research; E.B.-M. and A.C.S. analyzed data; E.B.-M., A.C.S., and G.M. wrote the paper.

This work was funded by National Institutes of Health Grants R01-MH-75702 to D.G.A. and OD-011107 to the California National Primate Research Center, and F32-MH-087067, which supported E.B.-M. We thank Alice Chou for help with data collection, and Mark Baxter and Vincent Costa for helpful feedback on a draft of the manuscript.

The authors declare no competing financial interests.

Correspondence should be addressed to Eliza Bliss-Moreau at eblissmoreau@ucdavis.edu.

https://doi.org/10.1523/JNEUROSCI.0673-21.2021

Neural activity in the ACC correlates with affective information during decision-making (Rushworth et al., 2004, 2007; Kennerley et al., 2009; Amemori and Graybiel, 2012; Chudasama et al., 2013; Enel et al., 2020), salience processing (Isomura et al., 2003), and autonomic control (Alexander et al., 2020). The ACC in nonhuman primates (NHPs) and humans coactivates with similar hubs in imaging studies (Vincent et al., 2007; Mantini et al., 2011; Touroutoglou et al., 2016), supporting the idea that the ACC contributes to similar network-level computations integrating affect with cognition and action across species (Rolls, 2019).

Despite pervasive correlations of ACC structure and function with affective measures, the causal relationship underlying these correlations remains elusive because of limited data from causal manipulations of the ACC such as lesions or local pharmacological manipulations in the context of behavior. Studies of focal damage to ACC, which range in the extent of damage to the ACC and surrounding areas and have primarily been created via aspiration, have demonstrated evidence of only minimal effects on cognitive tasks (Pribram and Fulton, 1954; Murray et al., 1989; Meunier et al., 1997; Parker and Gaffan, 1997; Rushworth et al., 2003). Instrumental tasks point to disrupted reward processing, particularly in the context of decision-making (Hadland et al., 2003a; Chudasama et al., 2013). Some reports indicate that following surgery compared with controls, ACC-lesioned monkeys were more aggressive (Mirsky et al., 1957) or less aggressive/more "tame" (Smith, 1944; Glees et al., 1950; Pribram and Fulton, 1954). When responsivity to the threat of snakes was tested, monkeys with damage to the area 24 and 32 in sulcus or gyrus) showed modest behavioral differences compared with control monkeys (Rudebeck et al., 2006).

To understand how selective ACC damage impacts affective reactivity, we tested rhesus monkeys who received neurotoxic ACC lesions or were neurologically intact on two threat-processing tasks—human intruder (HI; Kalin and Shelton, 1989; Gottlieb and Capitanio, 2013) and object responsiveness (OR; Bliss-Moreau et al., 2010, 2011). These tasks are thought to provide ground truth about the capacity of a monkey to generate affect-related behavior in the presence of stimuli that are ostensibly threatening. Variation in performance on these tasks has been shown, for example, to be related to amygdala structure (Izquierdo and Murray, 2004; Mason et al., 2006) and function (Fox et al., 2018), variation in estrogen (Bliss-Moreau and Baxter, 2018) and cortisol (Capitanio et al., 2011; Hamel et al., 2017), and the social environment of infants (Gottlieb and Capitanio, 2013). Both tasks are robust insofar as healthy normal monkeys show a stereotyped pattern of behavior across trial types and thus the absence or attenuation of effects provides a definitive indication that affective reactivity has been impacted by experimental manipulation, in this case the ablation of the ACC.

Materials and Methods

All procedures and methods were approved by the University of California, Davis, Institutional Animal Care and Use Committee.

Subjects

Fourteen adult male rhesus macaques were selected from seven large outdoor field enclosures (total area, 0.2 hectare; width, 30.5 m; depth, 61 m; height, 2.44 m; ~60–120 animals/cage) at the California National Primate Research Center (CNPRC) to participate in the current study. Monkeys were screened for normal social behavior before inclusion in the study (see below). One monkey from each enclosure was assigned to the control group, and one to the ACC lesion group. At ~4.78 years of age (SD = 0.58), monkeys moved indoors into standard caging (based on their weights: width, 59 cm; depth, 69 cm; height, 83 cm; or width, 87 cm; depth, 66 cm; height, 83 cm) and were pair housed either continuously or intermittently—a minimum of 7 h/d, 7 d/week—with the other animal selected from their field cage. One monkey from each pair received bilateral ibotenate lesions to the anterior cingulate cortex (see surgical details below) and the other was a control.

Monkeys were fed monkey chow twice daily, provided an oat-rice-pea enrichment once daily, a variety of fruits and vegetables biweekly, and water *ad libitum*. Monkeys had continuous access to Nylabones or Kong toys and standard CNPRC enrichment (e.g., videos of monkeys weekly). Rooms were maintained on a 12 h light/dark cycle at ~26°C.

Subject selection

Monkeys for this study were selected from their field cages after a series of 10 5 min focal observations (50 min total) were conducted to determine that they were socially integrated and had no stereotypies or other abnormal behaviors. These observations ensured that the monkeys that came from each field cage interacted prosocially and were not aggressive toward each other.

Once relocated indoors and paired, we conducted a series of behavioral observations on each pair (5 min focal observations for 15 observations total), including ratings of which monkey was dominant in the pairing. These data (G. Moadab, J. A. Charbonneau, E Bliss-Moreau, unpublished observation) were used to determine lesion group such that average social engagement (indexed by time spent in proximity, initiating grooming and other behaviors), affective reactivity, and dominance status (relative to behaviors like displacement, monopolizing of food/toys/other resources, avoidance and submissive signaling) were balanced across lesion groups. Serotonin transporter and MAOA (monoamine oxidase A) polymorphism genotypes were also balanced across group. Experimenters collecting behavioral data were blind to lesion condition.

Surgical procedures

Presurgical MRI and surgical planning. MRI scanning was conducted before each surgery at the UC Davis Veterinary Medical Teaching Hospital on a 1.5 T Genesis Signa MRI Scanner (GE Healthcare). Monkeys were sedated with ketamine and placed in an MRI-compatible stereotaxic apparatus (Crist Instrument) for imaging. Axial SPGR (spoiled gradient-recalled acquisition in a steady state) T1-weighted images were collected with a TR of 22 and a TE of 7.9, two averages were acquired with a flip angle of 30°, which resulted in a slice thickness of 1 mm and a resolution of 0.625 × 0.625 mm/voxel. Using Canvas X software (ACD Systems), T1 images in the coronal plane were overlaid with a scaled grid which was 1 × 1 mm. These images were used to determine the spatial position of the injection sites using the middle of the sagittal sinus and the surface of the brain as landmarks. Given that the cytoarchitecture boundaries of the caudal extent of the ACC are not visible on MRI, the boundary was set at the anteroposterior (AP) level of the rostral end of the anterior hippocampus in a coronal slice in which the hippocampal anatomy was completely visible in both the left and right hemispheres.

Surgeries were planned to have the lesion involve gyrus and ventral bank of the sulcus wrapping around the genu (areas 24 and 32) and including area 25 using the spatial definitions proposed by Vogt (2009, their Fig. 12), which do not include the dorsal bank, which is considered to be a motor area (Dum and Strick, 2002). Planning used the guideline that each 1 µl of ibotenate would spatially extend to ~1 mm^3 of cortex from the site of injection. Stereotaxic coordinates were computed from the MRI scans, and injections were planned for every 2 mm.

Surgery. Monkeys were sedated with ketamine hydrochloride (10 mg/kg, i.m.), had their heads shaved, and were endotracheally intubated. Monkeys were then anesthetized with a combination of isoflurane (~1%; mixed initially with oxygen and then with medical grade air) and fentanyl (7–10 µg/kg/h) via intravenous administration. Each monkey was placed in the same stereotaxic frame used for MRI acquisition. After surgical scrubbing and draping, a midline incision was made, and the skin, fascia, and muscle were separated into three layers. Dimensions for a single craniotomy extending ~3 mm beyond the proposed AP and

mediolateral (ML) coordinates were drawn onto the skull. Titanium clips with self-tapping bone screws (catalog #218–0201, #218–0217, #218–1604 using #220–0019, Osteomed) were placed on the interior of the bone flap, and the clips were shifted slightly out of position allowing the drill access to the skull. The bone flap was removed and was stored for the duration of the surgery in warm sterile saline. The dura was opened along the AP and ML extents of the craniotomy but was not removed from the midline.

Ibotenate (catalog # 0285, lots 26B/90 549 and 26C/100306, Tocris Bioscience) was prepared for injection at a concentration of 10 μg/μl in 0.22 μm sterile filtered 0.1 M PBS. Ibotenate injections were conducted using a micromanipulator (model 1760–61-SB, Kopf) fitted with 10 μl syringes (catalog #7531, Hamilton) with 7-cm-long, 26s (smaller inner diameter, thick-walled) gauge needles with a 30° bevel. Because the stereotaxic arms were so close to the midline, injecting both hemispheres simultaneously was not possible. Initially, we injected the entire left side (caudal to rostral) then the entire right side (rostral to caudal), and in later surgeries we alternated between injections on the right and left sides moving caudal to rostral. A total of 19–23 injections per hemisphere were performed to cover areas 32, 24, and 25.

Once injections were complete, the dura was moved into position covering the brain and sutured when possible. A layer of Surgicel (Ethicon) and GelFoam (GE Healthcare) was placed over the brain before the bone flap was repositioned. Self-tapping screws were placed in the titanium clips, which were already secured on the bone flap and tapped into the skull. The muscle, fascia, and skin were closed with sutures in their respective layers, and skin glue was used for final closing of the skin wound. Monkeys were removed from the stereotaxic frame and recovered in the postoperative suite at the CNPRC. The lesion surgeries ranged in length from 15.5 to 22.75 h (mean = 17.6 h; SD = 2.48).

Control animals underwent "sham" procedures during which they were sedated and anesthetized according to the procedures detailed above but only received midline incisions. In six of seven cases, their skulls were not opened. In one case, the skull of the animal was opened because the animal was an intended lesion subject. The control procedure was aborted when there was immediate significant brain swelling after opening the dura. He was treated with mannitol 25% (1.65–2.2 g/kg, i.v., over 20 min) and furosemide (1–4 mg/kg, i.v.) and hyperventilated to reduce brain swelling. When the brain returned to normal, the opening was closed as described above; the animal was maintained as a control animal and the pairmate was moved to the lesion group. Control animals were maintained under anesthesia for 8–12 h (mean = 10.4 h; SD = 1.49). This balanced a skin incision and prolonged general anesthesia, which might be reasonably expected to have some effect on behavior independent of ACC damage, with the practical constraints of fully matching anesthesia duration experienced by the ACC group.

Both lesion and sham subjects received 5 d of prophylactic antibiotic (cefazolin) after surgery (20 mg/kg, i.m.) as well as 3–5 d of treatment with an opiate (oxymorphone, 0.15 mg/kg, i.m.; buprenorphine, 0.01–0.03 mg/kg, i.m.) or a nonopiate analgesic (acetaminophen, 10–15 mg/kg, p.o.; ketoprofen, 1–2 mg/kg, i.m.) as needed and determined by the veterinary staff. Three lesion subjects received diuretics (mannitol 25%, 1.65–2.2 g/kg, i.v., over 20 min; furosemide, 1–4 mg/kg, i.v.) during surgery to relieve brain swelling; one of these animals also receive 4 d of treatment with dexamethasone (48 mg initial dose, halved three times) to avoid swelling postoperatively. One of the sham lesion subjects received diuretics during surgery (mannitol 25%, 1.65–2.2 g/kg, i.v., over 20 min; furosemide, 1–4 mg/kg, i.v.). One subject received a bronchodilator and additional analgesics (albuterol, 2.5 ml with 10 ml of 0.9% NaCl nebulized) and a second antibiotic (enrofloxacin, 10 mg/kg, i.m.) to relieve breathing complications.

The lesion versus control group assignment of all monkeys was maintained by Dr. Bliss-Moreau alone, and all technicians and researchers involved in data collection were blind to experimental conditions. In addition to ensuring that control monkeys had exposure to anesthesia that was similar to that of monkeys with ACC lesions, the midline incisions on all monkeys allowed technicians to be blind to conditions even during the recovery process.

Histologic procedures and lesion confirmation

At the conclusion of the study, monkeys in the ACC lesion group were killed with 0.33 ml/kg Fatal-Plus (120 mg/kg sodium pentobarbital; Vortech Pharmaceuticals) by a veterinary pathologist according to CNPRC standard operating procedures. Monkeys in the control group were not killed at the conclusion of the study. Instead, we used control tissue from another study (Grayson et al., 2017) for histologic analyses so as not to require the killing of otherwise healthy animals—we refer to these monkeys as the "histologic controls." At the time of killing, the lesion animals had an average age of 9.29 years (SD = 0.51), and the control animals had an average age of 11.75 years (SD = 0.83); the lesion animals averaged 16.38 kg in weight (SD = 1.99), and the control animals averaged 13.39 kg in weight (SD = 0.38).

Histologic and immunohistological processing was performed according to previously published methods (Lavenex et al., 2009). Monkeys were transcardially perfused with 1% paraformaldehyde (PFA) in 0.1 M sodium phosphate buffer at 4°C at a rate of 250 ml/min for 2 min followed by 4% PFA at a rate of 250 ml/10 min. For the last 50 min of the perfusion, the perfusion rate of 4% PFA was increased to 100 ml/min. The brain was then blocked caudal to the corpus callosum, extracted from the skull, and placed in 4% PFA for a 6 h postfix. Once postfixed, the brain was prepared for freezing by immersion in 10% glycerin with 2% dimethylsulfoxide (DMSO) in 0.1 M sodium phosphate buffer for 24 h, then 20% glycerin with 2% DMSO in 0.1 M sodium phosphate buffer for 72 h. The blocks of the brain were then frozen in 2-methyl-butane within a dry ice and ethanol bath. Using a freezing sledge microtome (model HM 440E, Microm International), the brain was sectioned at thicknesses of 30 and 60 μm. Sections were collected in a 1:7 series (six 30 μm sections and one 60 μm section) so that the brain could be evaluated every 240 μm for different histologic or immunohistologic stains.

The 60 μm series was used for Nissl staining. Sections were placed in 10% buffered formaldehyde for 2 weeks. Tissue was then rinsed twice in 0.1 M sodium phosphate buffer, and sections were mounted onto gelatin-coated glass slides and dried overnight. Dried sections were placed in a 1:1 mixture of chloroform and ethanol for 2 h, then in a fresh mixture of 1:1 chloroform, ethanol for another 2 h, and finally were partially hydrated and left overnight at 37°C. Sections were stained in 0.25% thionin (Thermo Fisher Scientific) for 35 s then dehydrated, decolored, cleared in xylene, and coverslipped with DPX Mountant (Electron Microscopy Sciences).

Sections for immunohistochemistry and long-term storage were placed in 1.5 ml microcentrifuge tubes in a tissue collection solution (TCS), consisting of 25% glycerol and 30% propylene glycol in 0.05 M phosphate buffer, and frozen at −80°C. One of the 30 μm series was used for immunohistochemistry. The series was removed from TCS after thawing and processed free floating in nets and bases. Tissue was rinsed for 3× 10 min in 1.5 Tris (which is 0.05 M Tris buffer + 1.5% NaCl), followed by a pretreatment of hydrogen peroxide solution 0.5% in 1.5 Tris for 15 min with rotation to reduce endogenous peroxidases activity. Sections were rinsed and then blocked in 0.5% Triton X-100 (TX-100) and 10% normal horse serum (NHS) in 1.5 Tris for 4 h. After blocking, tissue was incubated for 48 h in monoclonal anti-SMI-32 (1:2000; catalog #801701, BioLegend), 0.3% TX-100, and 1% NHS in 1.5 Tris. Postincubation, sections were rinsed and incubated in biotinylated horse anti-mouse IgG (catalog #BA-2000, Vector Laboratories) at 1:227, 0.3% TX-100, 1% NHS in 1.5 Tris, then rinsed and reacted with avidin-biotin (ImmunoBioScience) at 1:200 and 1:100, for parts A and B, respectively. Incubations in biotinylated secondary solutions and avidin-biotin solutions were repeated to increase enzymatic activity. Sections were then reacted with 0.05% diaminobenzidine (catalog #D9015, Sigma-Aldrich) with 0.04% hydrogen peroxide. Sections were mounted on gelatin-coated slides, dried overnight, defatted twice in mixtures of 1:1 chloroform and ethanol for 2 h, dehydrated and cleared in xylene, and coverslipped with DPX Mountant. Tissue from lesioned animals and histologic control animals was processed together to eliminate batch processing differences.

Lesion analysis

Lesion analysis was performed using the Nissl-stained tissue series and the series stained for SMI-32 immunohistochemistry. Nissl- and SMI-32-stained slides were scanned using a TissueScope scanner (Huron Digital Pathology), and images were imported into StereoInvestigator

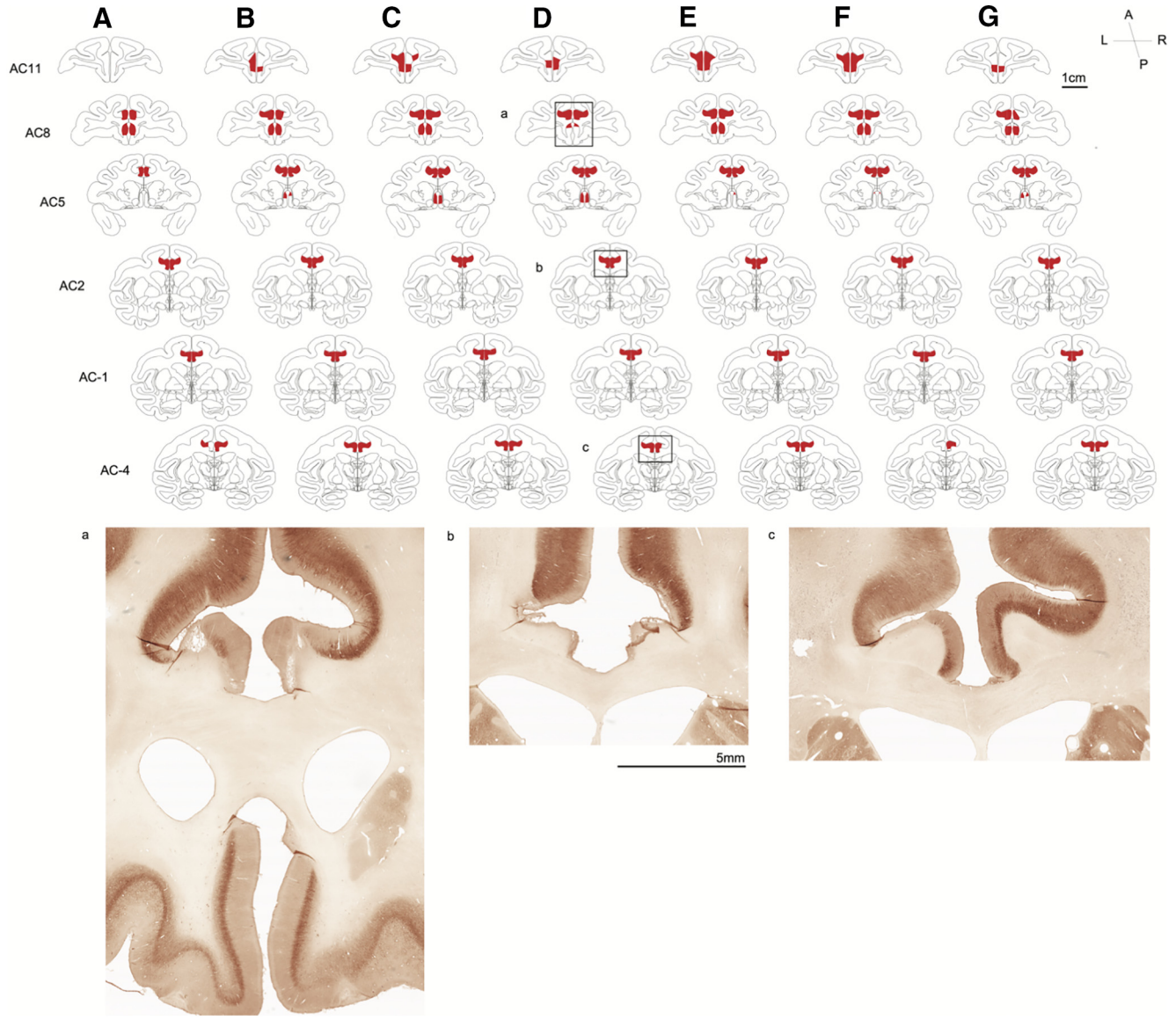

Figure 1. Representations of lesion extent (red) were made by overlaying the StereoInvestigator tracings over templates for the macaque brain, which were made using http://braininfo.rprc.washington.edu/PrimateBrainMaps/atlas/Mapcorindex.html. ***A–G***, Each column is a separate monkey. The rows are drawings of coronal sections arranged from rostral (top) to caudal (bottom). Sections are separated by 3 mm, and the distance from the anterior commissure (AC) is indicated (e.g., AC2 is ~2 mm rostral to the AC and AC-4 is ~4 mm caudal to the AC). Images ***a–c*** are examples of SMI-32 Immunochemistry scanned images, which were used for evaluation of the lesion area for each 30 μm section.

(version 2020.1.3, MBF Bioscience). Lesion estimation and/or ACC volume estimation were conducted on sections every 480 µm. Areas 24, 32, and 25 were traced first in control cases referring to existing documentation of their structure (Vogt et al., 2005). In lesion cases, cortex was traced only if there were cells present and the layering of the cortex appeared intact. Areas were traced on the Nissl-stained sections, and the tracer was able to flip between the Nissl-stained and the SMI-32-stained sections when necessary. Both Nissl- and SMI-32-stained sections were used to determine lesion extent/ACC volume because in lesion cases where tissue has been damaged it was nearly impossible to determine the boundaries between areas 24, 32, and 25 (which are based largely on the distribution of neurons) on only the Nissl-stained sections. Visualizing the distribution of neurons using SMI-32-stained tissue helped to ensure accuracy of our analysis. Volume measurements were made using the Cavileri estimator in StereoInvestigator with a grid size of 100 × 100 µm with a *z*-interval of 480 µm. The mean volume of the control monkeys was then compared with the volume of remaining viable cortical volume in monkeys with ACC lesions and reported as a percentage (Fig. 1).

Behavioral affective reactivity experimental procedures

Following a recovery period after surgery, monkeys participated in two experiments to assess affective processing and reactivity. Monkeys were tested on two standard evaluations of behavioral responsivity to threat for NHPs: the human intruder task (Kalin and Shelton, 1989; 1998; Gottlieb and Capitanio, 2013; Bliss-Moreau and Moadab, 2016.) and the object responsiveness task (Prather et al., 2001; Bliss-Moreau et al., 2010, 2011).

Human intruder (HI)

Monkeys were 6.40 years old (SD = 0.56) at the time of HI testing. Monkeys were tested Monday to Friday on 5 consecutive days between 1:00 and 3:00 P.M. On each test day, monkeys were moved one at a time from their home cages to a test room into a standard primate cage (width, 85.5 cm; depth, 68 cm; height, 82 cm) with no perch bar. After a brief 1 min acclimation, an unfamiliar human entered the room and presented himself to the monkey for 1 min intervals in four different positions (4 min total). The various positions were presented in the following order: (1) *profile-far*, human standing 1 m from cage facing 90° away from the cage; (2) *profile-near*, human standing 0.3 m from the cage,

Table 1. Behavioral ethogram

Behavior	Description	HI	OR
Bark	Low pitched, sharp, guttural sound	X	
Bared teeth	Exaggerated movement of lips such that lips are pulled back with teeth showing	X	X
Cage shake	Vigorous shaking of cage bars or body slams against the cage	X	X
Coo	Clear, soft sounds, moderate in pitch and intensity; usually sounds like "whoooooo..."	X	
Freeze	Stiff body posture without any movement for more than three seconds	X	X
Grunt	Deep, muffled, low-intensity vocalization	X	X
Lipsmack	Rapid lip movements with pursed or puckered lips, usually accompanied by smacking sounds	X	X
Scratch	Scratching own body	X	X
Scream	High-pitched vocalization, with extreme high intensity; sounds like "eeeeeeeeee..."	X	
Self-groom	Examining, picking, or licking own fur or skin	X	
Self-shake*	Full body shaking	X	
Stereotypy	Repetitive motor or abnormal behavior	X	X
Tooth grind	Repetitive, audible rubbing of upper and lower teeth	X	X
Threat	Facial behavior in which one or more of the following components are exhibited with elevated intensity in the stare: open mouth stare, head bobbing, ear flaps, or lunges	X	X
Yawn	Wide opening of the mouth while inhaling deeply	X	X

*Self-shake was the only behavior that was not on the ethogram for human intruder. It is possible that the behavior occurred but was not coded.

facing 90° away from the cage; (3) *stare-far*, human standing 1 m from the cage, facing the cage, and making eye contact with the subject; and (4) *stare-near*, human standing 0.3 m from the cage, facing the cage, and making eye contact with the subject.

A trained observer standing 45° to the right of the animal scored behaviors of interest during the task using a standardized ethogram that recorded position in the cage and affect-related behaviors using a 1/0 scoring method and 10 s bins (a modification of the procedure from the study by Capitanio, 1999). Behaviors that were recorded are outlined in Table 1. If a behavior was present within a given 10 s bin, that behavior received a score of 1 for that bin. If a behavior was not present for a given 10 s bin, that behavior received a score of 0 for that bin. This type of scoring, rather than "all occurrence" scoring, allows behavioral data to be scored live, which has the advantage of being able to capture subtle behaviors that cannot be seen or heard on video. Behaviors were summed into an index representing affective reactivity for each trial type on each day. Live scoring was conducted by one observer who had an interrater reliability with the laboratory trainer of 90%.

Object responsiveness

At ~6.61 years of age (SD = 0.52 years), subjects were tested on the OR task. On each day of testing, subjects were moved from their home cage to a test cage in a separate room. The test cage was a modified baboon cage (depth, 83.32 cm; height, 101.6 cm; width, 80.01 cm) with a clear front containing two vertical openings (height, 25 cm; width, 5 cm) separated by 5.08 cm through which the monkey could reach. A platform secured to the front of the test cage contained a food well (depth, 2.54 cm; width, 2.54 cm; ~5.18 cm from the front of the test cage) in which food items could be placed, and behind that a recessed rectangle (depth, 22.86 cm; width, 15.24 cm) in which test objects mounted on a board of the same size could be placed and locked in place. An opaque plastic panel in front of the clear sheet ran along vertical tracks, operated by a rope-and-pulley system. Experimenters could lower the opaque panel using the rope to shield the food item and object from view of the animal between trials. Monkeys were acclimated to the test cage before beginning testing.

Each monkey completed 10 d of testing, Monday to Friday, across 2 consecutive weeks. Monkeys were presented with two object types (10 ostensibly threatening animal objects and 10 neutral objects), each in two forms, simple and complex (resulting in 40 objects total). Generally, two of each object were purchased, and one of each set was altered to become the simple version of the object. To create the simple form of each object, distinguishing textures and facial features from the complex objects were eliminated, either by smoothing gray clay or plaster bandage (typically used for orthopedic casting) over the object or simply by spray painting the object gray. In a few cases, objects were painted green (e.g., the cheese grater) to standardize color across the set and to eliminate nonbiological colors (like metal). Additionally, the simple version of the green golf balls was ping pong balls spray painted gray. All objects were novel to the animals. The objects were variable in size (largest: length, 66 cm; width, 22.86 cm; height, 7.62 cm; smallest: length, 12.7 cm; width, 5.08 cm; height, 6.35 cm; Fig. 2, objects).

On each test day, animals were presented nine total trials of two trial types—food-only trials (trials during which food reward was presented alone: odd trials) and object trials (trials during which a food reward was presented in front of an object: even trials). This resulted in a total of 90 trials—40 object trials and 50 food-only trials. Both control and animal-like objects were presented on each test day, in both simple and complex forms. Simple and complex forms of the same object were presented back-to-back, separated by a food-only trial (i.e., simple form of snake, food-only trial, complex form of snake). Trials were 30 s in length.

On the first day of testing, the first object type presented was always a neutral object. On subsequent days, object type was counterbalanced so that either object type could be presented first. Object types and forms were counterbalanced across test days and were arranged into two presentation orders. Presentation orders were assigned to subjects pseudorandomly, balancing across the lesion condition. The primary dependent variables (i.e., latency to retrieve food reward and exploration of the objects) as well as other species-typical behaviors (Table 1) were recorded live using The Observer (Noldus).

A trained observer scored behaviors of interest in real time using a standardized ethogram that recorded all occurrences of affect-related behaviors (Table 1). As with HI data, behaviors were summed into an index representing affective reactivity for each object type and complexity.

Data analysis

Data analysis was conducted in R version 4.0.3 (R Core Team, 2019). Generalized linear mixed-effects models implemented in the *lme4* package (Bates et al., 2014) were used to model affective reactivity, accounting for within-subject clustering of observations by incorporating a random intercept for each subject. The *DHARMa* package (Hartig, 2020) was used to generate Q-Q plots for the fitted model residuals against simulated residuals to evaluate model fit for selecting appropriate glms (e.g., negative binomial vs Poisson) and for detecting outliers. We report the results of type II anovas using the *Anova* function in the *car* package (Fox and Weisberg, 2019) when reporting the main effects and interactions. The *emmeans* package (Lenth, 2020) was used to compute estimated marginal means and parameters of interest (e.g., slopes in reactivity across days for each lesion condition) in cases of interactions. We note that negative binomial regression models were found to best fit the reactivity data. We report the rate ratios (RRs) from these models, which reflect the multiplicative factor by which average reactivity counts differed between independent variables of interest. RRs <1 indicate that mean reactivity counts were lower in the indicated group compared with

the reference level, and RRs >1 indicate that reactivity was higher in the indicated group compared with the reference level.

Latency data were analyzed using mixed-effects Cox proportional hazards models with a random intercept for each subject using the *coxme* package (Therneau, 2020). Observations of the indicated behavior (e.g., "latency to take treat") were censored at the duration of the trial (30 s) if the animal did not engage in the indicated behavior during the trial. We report hazard ratios (HRs) from these models—HRs <1 indicate that animals took longer to engage in the indicated behavior (e.g., "take treat"), and HRs >1 indicate that animals were engaged in the indicated behavior more quickly.

All inference was conducted with a two-sided significance level of $\alpha = 0.05$, and 95% CIs are provided where appropriate.

We note that, as is the case with all NHP research, the sample size here is small, which makes the variance between subjects potentially more impactful than if the sample size was much larger. Two of the control animals were particularly reactive, especially during the human intruder task; however, these data points were not found to be outliers using the *testOutliers* function provided in the DHARMa package (Hartig, 2020) and thus may not be greatly influencing the findings.

Results

Lesion confirmation

Histologic analyses demonstrated significant neuron loss and atrophy to the ACC in lesioned animals, as expected, with some variation across region (areas 24, 32, and 25). Importantly, calculations of damage are inherently relational to our control animals given that we used the volumes of their ACC to compute the percentage of atrophy in our lesioned animals. This is critical to note because one of our control animals (control 3) had smaller ACC volumes compared with the other two control animals (control 1 and 2) and artificially decreased the computations of tissue spared for some of our lesioned animals. That is, when we computed tissue spared for case A and case G, there was essentially no damage to area 32, although damage was observed during histologic evaluation. This is because the volume of the tissue spared was greater than that of area 32 in control cases (this is particularly true for case A). We could have adopted an alternative strategy and compared our lesioned cases to an atlas, but atlases are typically based on single cases, and rarely is contextual information about the animal provided (e.g., rearing history, social housing history); we believe that using multiple control cases where that contextual information is known is a better approach. We also note that we opted for a conservative approach to the computations of tissue spared, including any neurons as "spared" even if they sat in isolated islands (typically in superficial layers, with deeper layers destroyed), which may also decrease the atrophy values. Case-by-case schematics of tissue damage from visual inspection are presented in Figure 1 and detail nearly complete damage across the lesion group.

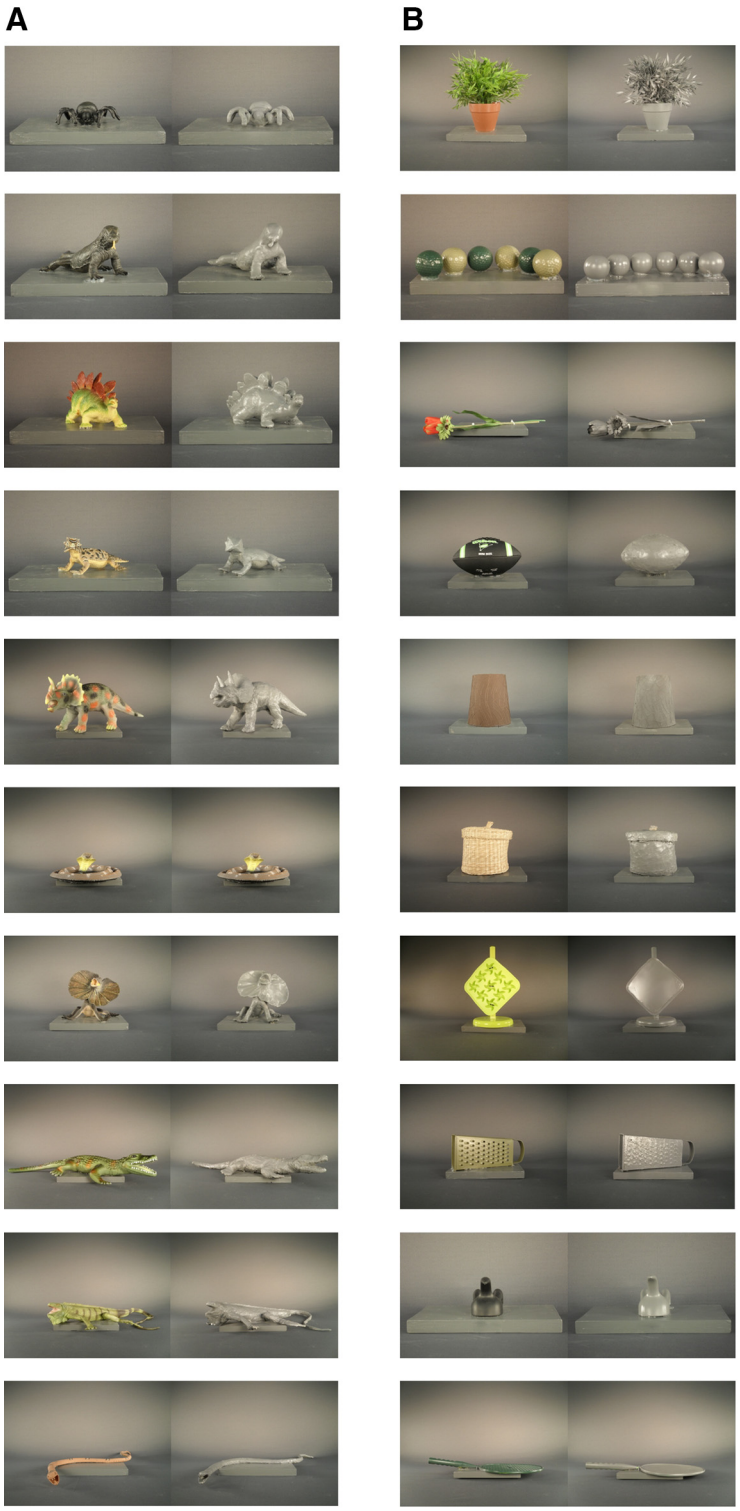

Figure 2. Objects used in Object Responsiveness testing. ***A***, Ostensibly threatening objects which served as stimuli. ***B***, Neutral objects which served as stimuli. Left panels of each column are the complex form and right panels of each column are the simple form. Scale is provided by the blocks to which objects were attached, which were identical in size (4 × 7 inches).

Atrophy to area 24 was the most extensive and consistent for the lesion group, with nearly all animals sustaining extensive bilateral damage. When tissue was spared, it consisted of islands of cells that were isolated and localized in patches directly above the white matter, and in a few cases some sparing of cortical layering in the superficial layers (with deep layers gone) or the

Table 2. Size of ACC subregions in histologic controls and ACC-lesioned animals

	Area 24				Area 32				Area 25			
	Left Volume	Right Volume	Left Atrophy	Right Atrophy	Left Volume	Right Volume	Left Atrophy	Right Atrophy	Left Volume	Right Volume	Left Atrophy	Right Atrophy
Control animals												
Control 1	211.78	216.07			63.04	62.64			20.54	19.30		
Control 2	275.77	258.80			64.62	83.63			24.34	22.14		
Control 3	205.52	224.35			47.99	46.13			30.43	30.77		
Control average	*230.88*	*233.07*			*58.55*	*64.13*			*25.10*	*24.07*		
ACC-lesioned animals												
Case A	130.83	99.24	*43.33%*	*57.42%*	85.91	83.78	*0%*	*0%*	18.89	20.81	*24.77%*	*13.57%*
Case B	63.69	54.40	*72.43%*	*76.66%*	46.26	45.65	*21.00%*	*22.03%*	2.09	8.12	*91.67%*	*66.26%*
Case C	12.61	13.54	*94.54%*	*94.19%*	29.83	24.03	*49.06%*	*62.53%*	7.13	8.06	*71.60%*	*66.51%*
Case D	22.99	43.32	*90.04%*	*81.41%*	37.06	50.10	*36.71%*	*21.88%*	17.06	10.01	*32.05%*	*58.41%*
Case E	23.11	20.29	*89.99%*	*91.29%*	18.56	18.71	*68.31%*	*70.83%*	7.39	5.34	*70.55%*	*77.82%*
Case F	41.10	25.64	*82.20%*	*89.00%*	25.49	20.99	*56.46%*	*67.27%*	8.76	15.45	*65.12%*	*35.84%*
Case G	40.12	72.99	*82.62%*	*68.68%*	44.15	63.40	*24.59%*	*1.15%*	17.30	7.50	*31.08%*	*68.82%*
ACC-lesioned average	*47.78*	*47.06*	*79.31%*	*79.81%*	*41.04*	*40.54*	*36.59%*	*35.10%*	*11.23*	*11.76*	*55.26%*	*55.32%*

Volumes are in cubic millimeters. Measured values are in standard font and calculated values are in italics. The percentage of atrophy was calculated by hemisphere, as follows: (average volume for control animals – volume of each individual ACC-lesioned animal)/average volume for control animals. Calculations were computed in cubic microns and converted to cubic millimeters, then rounded to two decimal places.

deep layers (with superficial layers gone). That is, even in cases where tissue was spared, it did not appear to be normally organized or healthy. All monkeys with ACC lesions had some major damage to area 25, although there was greater variability in the tissue sparing than in area 24. Area 32 sustained the least consistent damage across monkeys. Area 32 of case A was essentially completely spared, and its volume was larger than that of the histologic controls. Case B had only minor atrophy bilaterally in area 32; the right side of area 32 I animal G also had significant sparing. The mean area 24 damage was 79.6% (SD = 14.4%). Mean area 32 damage was 39.9% (SD = 27.3%). Mean area 25 damage was 57.3% (SD = 21.9%; Table 2).

Tissue damage was fairly specific to the ACC, and when damage extended beyond the ACC it was limited to narrow, adjacent regions. Animals B, E, and F had some atrophy in the deep layers of the rostral medial orbital sulcus (at the junction of areas 11 and 13). There was also atrophy just dorsal to the cingulate sulcus in presupplementary motor area in animals B, C, F, and G. Animals B and C had atrophy in area 10 ventral to area 32. Animal B also had atrophy ventral to the targeted region in area 24, as well as minor atrophy to the rostral extent of area 23.

Human intruder

Across all trial types, affective reactivity data were skewed with a disproportionate number of low reactivity scores. Interrogation with the package *fitdist* (Delignette-Muller and Dutang, 2015; including evaluation of the density composition, Q-Q, and P-P plots) indicated that the data best fit a negative binomial distribution, which was confirmed when the residuals of the models were evaluated using the DHARMa package. A negative binomial generalized linear mixed model with trials nested within monkeys, trial type specified as a categorical variable, and lesion × trial type and lesion × test day interactions were conducted using *lme4*. Model statistics were generated using *Anova* in *car*, and estimated marginal means were generated using *emmeans* and were used to interpret the patterns of both main effects and interactions.

There was a significant effect of test day such that affective reactivity decreased across the test days for all animals ($\chi^2(1) = 40.55$, $p < 0.001$), and a significant effect of trial type such that all animals were more reactive in the stare compared with the profile conditions ($\chi^2(3) = 147.74$, $p < 0.001$). There was also a

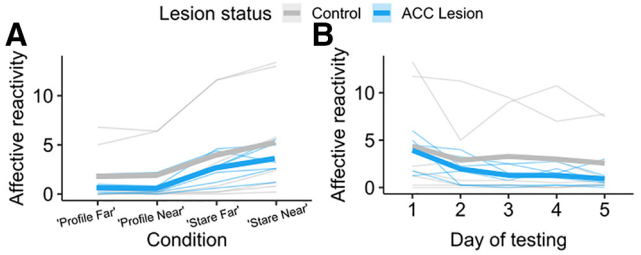

Figure 3. Affective reactivity in the Human Intruder task. ***A***, A significant lesion × condition interaction ($p = 0.032$) revealed that monkeys with ACC lesions were slightly less reactive in profile and stare conditions but still calibrated their reactivity in an appropriate manner. Despite the significant interaction, the reactivity of controls and monkeys with ACC lesions did not significantly differ in any of the individual conditions. ***B***, Monkeys with ACC lesions reduced affective reactivity across test days at an accelerated rate compared with controls ($p = 0.0001$).

significant lesion × trial type interaction ($\chi^2(3) = 8.81$, $p = 0.032$) and lesion × test day interaction ($\chi^2(1) = 14.74$, $p < 0.001$). Specifically, monkeys with ACC lesions were slightly less reactive in the profile conditions and increased their reactivity in the stare conditions more so than controls (Fig. 3*A*). Relative to the "profile far" condition, reactivity of controls did not differ significantly in the "profile near" condition [RR = 1.04 (95% CI, 0.64, 1.69), $z = 0.20$, $p = 0.98$], but was higher in "stare far" [RR = 2.24 (95% CI, 1.45, 3.45), $z = 4.37$, $p < 0.001$] and "stare near" [RR = 3.29 (95% CI, 2.15, 5.03), $z = 6.62$, $p < 0.001$] conditions. Relative to the profile far condition, the reactivity of monkeys with ACC lesions did not differ significantly in the profile near condition [RR = 0.88 (95% CI, 0.42, 1.86), $z = -0.40$, $p = 0.93$], but was higher in stare far [RR = 4.0 (95% CI, 2.23, 7.710, $z = 5.61$, $p < 0.001$] and stare near [RR = 5.65 (95% CI, 3.20, 9.98), $z = 7.17$, $p < 0.001$] conditions. Reactivity decreased across test days for both controls [RR = 0.90 (95% CI, 0.83, 0.97), $z = -2.50$, $p = 0.013$] and monkeys with ACC lesions [RR = 0.69 (95% CI, 0.62, 0.77), $z = -7.00$, $p < 0.001$]; reactivity decreased more rapidly across test days in monkeys with ACC lesions than in controls [$\beta = 0.77$ (95% CI, 0.67, 0.88), $z = 3.84$, $p < 0.001$; Fig. 3*B*]. The main effect of lesioning was not significant ($\chi^2(1) = 0.26$, $p = 0.61$). In sum, overall levels of reactivity were similar across experimental groups, and all animals were more responsive to the stare compared with the profile conditions. Both groups of

animals decreased their reactivity over test days; the reactivity of ACC-lesioned animals decreased more rapidly over test days than did that of controls.

Object responsiveness: affective reactivity

We first modeled lesion-related differences in affective reactivity on trials in which animals saw one of the objects (either neutral or animal) at either level of complexity (simple, complex) across test days. As in the HI data, affective reactivity was skewed to the right with a disproportionate number of low reactivity scores, and evaluation via the *fitdist* package (as described above) revealed that the negative binomial distribution was the best fit; residuals were checked to confirm this. A generalized linear mixed model with trials nested within subjects, trial type (neutral or animal), and complexity (simple or complex) specified as a categorical variable, and lesion × trial type, and lesion × complexity and lesion × test day interactions was conducted using *lme4*. Model statistics were generated using *Anova* in the *car* package and were estimated marginal means generated using *emmeans* and used to interpret the pattern of both main effects and interactions.

As expected, the animals were more reactive to animal stimuli than neutral stimuli and within the animal category more reactive to complex compared with simple stimuli, as evidenced by a significant interaction between stimulus category and complexity ($\chi^2(1) = 7.46$, $p = 0.0063$). Animals were nearly twice as reactive to complex compared with simple animal stimuli [RR = 1.91 (95% CI, 1.43, 2.54), $z = 4.40$, $p < 0.001$; Fig. 4*A*]. Complexity did not impact the neutral condition [RR = 1.04 (95% CI, 0.76, 1.44), $z = 0.26$, $p = 0.80$]. A follow-up test demonstrated that this relationship was not modified by lesion status (likelihood ratio test, $\chi^2(3) = 0.25$, $p = 0.97$). There was also a significant interaction between lesion condition and test day, such that monkeys with ACC lesions decreased reactivity across test days more so than controls ($\chi^2(1) = 13.13$, $p < 0.001$). Specifically, on average, the reactivity of controls did not significantly change from day to day [RR = 1.031 (95% CI, 0.98, 1.09), $z = 1.18$, $p = 0.24$], while the reactivity of monkeys with ACC lesions decreased significantly over test days [RR = 0.90 (95% CI, 0.86, 0.95), $z = -3.92$, $p < 0.001$; Fig. 4*B*]. As in the HI data, ACC lesions did not disrupt the overall levels of affective reactivity or calibration to levels of threat, but did impact the ability to sustain reactivity over test days.

Last, there were no lesion- or test day-related differences in affective reactivity during food-only trials: lesion ($\chi^2(1) = 0.27$, $p = 0.60$), test day ($\chi^2(1) = 1.44$, $p = 0.23$), or lesion × test day ($\chi^2(1) = 0.25$, $p = 0.62$), suggesting that the differences observed in responding when monkeys were tested with the objects were specific to their processing of the objects.

Object exploration

Given the results above, we fit a mixed-effects Cox proportional hazards model on latency to explore the presented object on a given trial, and included a two-way interaction between stimulus complexity and stimulus type and a two-way interaction between lesion condition and test day in the model. There was a main effect of stimulus category ($\chi^2(1) = 70.5$, $p < 0.001$), but no main effect of stimulus complexity ($\chi^2(1) = 1.33$, $p = 0.25$), lesion condition ($\chi^2(1) = 0.25$, $p = 0.62$), or day of testing ($\chi^2(1) = 0.88$, $p = 0.35$). Consistent with the reactivity analysis above, we observed a significant interaction between stimulus type and complexity in latency to explore the object, such that monkeys more readily explored complex neutral objects but less readily explored complex animals ($\chi^2(1) = 4.76$, $p = 0.029$). Specifically, while stimulus complexity of neutral objects did not significantly alter the speed with which monkeys explored these objects [complex vs simple: HR = 1.4 (95% CI, 0.98, 2.0), $z = 1.87$, $p = 0.06$], and while monkeys were not significantly slower to explore complex animal stimuli relative to simple animal stimuli (complex vs simple: HR = 0.47 95% CI, 0.19, 1.18), $z = -1.61$, $p = 0.11$], these effects trended in opposite directions, leading them to be significantly different ($\chi^2(1) = 4.76$, $p = 0.029$). Lesion condition did not significantly modify this effect (likelihood ratio test: $\chi^2(3) = 3.10$, $p = 0.38$). Similarly, consistent with reactivity analyses above, we observed a significant lesion by test day interaction ($\chi^2(1) = 3.90$, $p = 0.048$) such that controls accelerated the rate with which they explored objects across test day [HR = 1.10 (95% CI, 1.005, 1.20), $z = 2.07$, $p = 0.038$] whereas monkeys with ACC lesions did not alter the rate with which they explored objects across test day [HR = 0.97 (95% CI, 0.89, 1.06), $z = -0.70$, $p = 0.483$].

Further, we assessed the degree to which lesion status affected the frequency with which monkeys explored the objects (Fig. 5). Following the results above, we fit a negative binomial generalized linear mixed model regressing the number of times monkeys explored the presented object on trial type (neutral or animal),

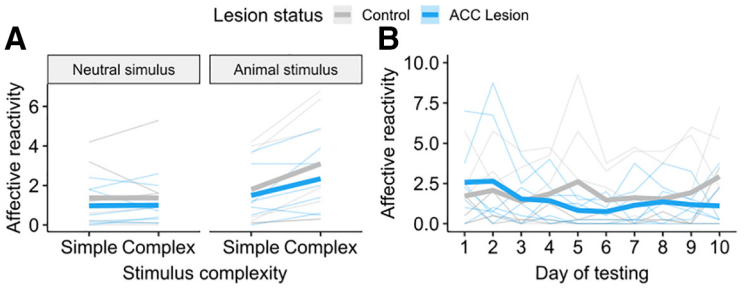

Figure 4. Affective reactivity in the Object Responsiveness Task. ***A***, Monkeys were no more reactive toward complex compared with simple neutral stimuli. Monkeys were more reactive toward complex relative to simple animal stimuli. ACC lesion status did not modify this association ($p = 0.97$). ***B***, Monkeys with ACC lesions reduced affective reactivity toward novel stimuli across test days at an accelerated rate compared with controls whose reactivity was essentially stable across test days ($p = 0.0002$).

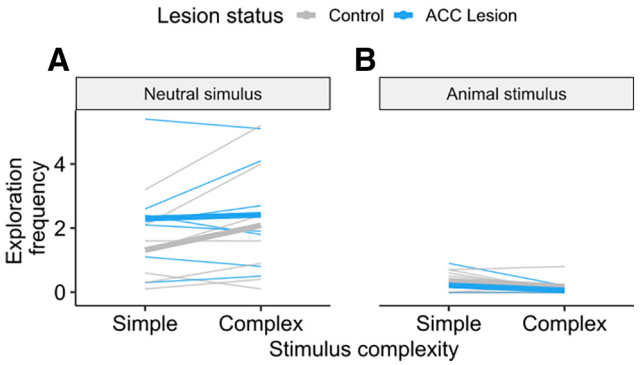

Figure 5. Frequency of exploring object stimuli. ***A***, ***B***, Both controls and monkeys with ACC lesions more readily explored neutral stimuli (***A***) relative to animal (***B***) stimuli ($p < 0.0001$). Stimulus complexity of neutral stimuli did not significantly alter the frequency of exploration ($p = 0.37$); however, both ACC lesion and control animals explored complex animal stimuli less frequently than simple animal stimuli ($p = 0.025$).

complexity (simple or complex), lesion × trial type, lesion × complexity interaction, and lesion × test day interaction. The results of this model demonstrated a main effect of stimulus category ($\chi^2(1) = 105.5$, $p < 0.001$), such that monkeys were less likely to explore animal stimuli overall, and a complexity × category interaction ($\chi^2(1) = 5.75$, $p = 0.017$), such that monkeys explored complex versus simple neutral objects at similar rates [RR = 1.23 (95% CI, 0.77, 1.99), $z = 0.89$, $p = 0.37$] but explored complex animal stimuli less than simple animal stimuli [RR = 0.41 (95% CI, 0.19, 0.89), $z = -2.27$, $p = 0.025$]. Further, there was evidence that lesions modified the association among stimulus type, stimulus complexity, or their interaction and exploration frequency (likelihood ratio test: $\chi^2(3) = 8.24$, $p = 0.041$). Specifically, while both controls and monkeys with ACC lesions explored animal stimuli less readily than neutral stimuli [lesion: HR = 0.15 (95% CI, 0.08, 0.27), $z = -6.23$, $p < 0.001$; control: HR = 0.039 (95% CI, 0.031, 0.19), $z = -8.39$, $p < 0.001$], this reduction in the exploration frequency of animals compared with neutral stimuli was significantly larger for monkeys with ACC lesions compared with controls ($z = -2.25$, $p = 0.025$). The main effects of stimulus complexity ($\chi^2(1) = 0.18$, $p = 0.67$), day of testing ($\chi^2(1) = 2.70$, $p = 0.10$), lesion ($\chi^2(1) = 0.041$, $p = 0.84$), and the interaction between lesion and test day ($\chi^2(1) = 0.14$, $p = 0.17$) were not significant.

Food retrieval behavior

We also assessed the degree to which lesion condition and stimulus type influenced the latency to retrieve food during trials on which stimuli were presented. We included an interaction between lesion status and test day and an interaction between stimulus complexity and stimulus type in the model. Stimulus complexity and stimulus type affected latency to retrieve food, indicating the sensitivity of this behavior to the nature of the stimuli, but behavior did not differ between controls and monkeys with ACC lesions. There were significant main effects of stimulus complexity, such that monkeys more readily retrieved food on simple versus complex trials ($\chi^2(1) = 13.9$, $p < 0.001$; Fig. 6). Further, there was a main effect of stimulus type such that monkeys were slower to retrieve treats when presented with an animal stimulus compared with a neutral stimulus ($\chi^2(1) = 28.9$, $p < 0.001$). However, there was a significant interaction between stimulus complexity and stimulus type ($\chi^2(1) = 17.24$, $p < 0.001$), such that the complexity of neutral objects did not significantly affect the speed with which monkeys retrieved food [complex vs simple: HR = 0.89 (95% CI, 0.65, 1.24), $z = -0.68$, $p = 0.50$], but monkeys were slower to retrieve food when a complex animal stimulus was presented compared with when a simple animal stimulus was presented [complex vs simple: HR = 0.27 (95% CI, 0.17, 0.43), $z = -5.55$, $p < 0.001$]. Lesion status did not significantly modify this effect (likelihood ratio test: $\chi^2(3) = 3.47$, $p = 0.33$). There was no main effect of lesion status ($\chi^2(1) = 0.34$, $p = 0.56$) and no evidence of an interaction between lesion status and test day ($\chi^2(1) = 0.097$, $p = 0.76$) on latency to retrieve food; however, there was a main effect of test day such that monkeys retrieved treats progressively quicker as days advanced [HR = 1.16 (95% CI, 1.10, 1.21), $z = 6.18$, $p < 0.001$].

We additionally fit a mixed-effects Cox model on latency to retrieve food on food-only trials and included lesion condition, test day, and their interaction in the model. There was a significant main effect of test day such that monkeys retrieved treats progressively quicker as testing continued over test days ($\chi^2(1) = 52.6$, $p < 0.001$). There was no main effect of lesion condition on latency to retrieve treats ($\chi^2(1) = 0.77$, $p = 0.34$). Controls retrieved the food reward 1.10 times quicker on each progressive day [HR = 1.10 (95% CI, 1.05, 1.15), $z = 3.74$, $p = 0.002$] and monkeys with ACC lesions retrieved the food reward 1.16 times quicker on each progressive day [HR = 1.16 (95% CI, 1.11, 1.22), $z = 6.53$, $p = 0.002$], though the difference in these acceleration rates to retrieve treats did not differ significantly between lesion conditions ($\chi^2(1) = 3.44$, $p = 0.06$).

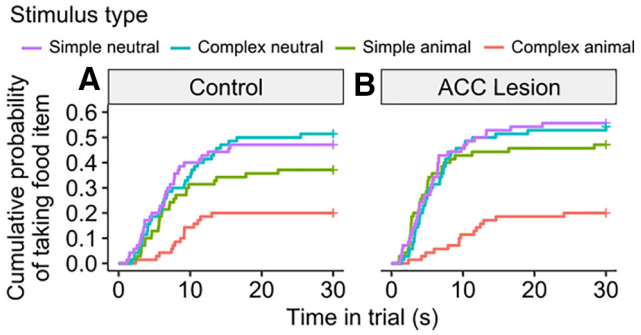

Figure 6. ***A***, ***B***, Empirically observed cumulative probabilities of taking food items in the presence of novel object stimuli in control (***A***) and ACC lesion (***B***) animals. Stimulus type and complexity modified the latency to take a food item in the presence of novel object stimuli ($p < 0.0001$). Monkeys were fastest to retrieve a food item in the presence of simple neutral object stimuli and slowest to retrieve food in the presence of complex animal object stimuli. Lesion status did not affect this trend ($p = 0.33$).

Discussion

Across two experiments, extensive damage to the ACC resulted in a perturbation of affective reactivity to threat. Monkeys with ACC damage initially responded to stimuli like controls, but over time their reactivity decreased more than controls—that is, ACC-lesioned animals were unable to sustain the magnitude of their response (vigor) over the time (vigilance). The interaction between lesion condition and time was consistent across experiments, although the threat types differed, and the same threat was repeated during human intruder, while different, ostensibly threatening objects were presented each day during object responsiveness. In both tasks, monkeys with ACC lesions calibrated their responses appropriately to different threat magnitudes, responding more robustly to the most potent threats and least robustly to the least potent threats or neutral stimuli. This calibration was observed in affect-related behaviors, object exploration, and food retrieval behavior. Overall, the robustness of responses to threat in monkeys with ACC lesions was comparable to that of control monkeys. This indicates that although the ACC is dispensable for appropriate calibration of affective responding, it is required to sustain the vigor of affective reactivity over time. This is congruent with the broad implication of the ACC in affective and emotional reactivity (for review, see Bush et al., 2000; Lindquist et al., 2012; Rolls, 2019) and particularly reactivity related to threat (Roberts, 2020). Data from the current study refine the understanding of the role of the ACC in these processes.

Like other cortical structures, primate ACC differs from rodent ACC both in terms of structure and connectivity in crucial ways. Although both the primate ACC and putatively homologous regions in rodents (Laubach et al., 2018) show some similarities in local cytoarchitecture and connectivity (Vogt et al., 2013; Vogt and Paxinos, 2014), the primate brain possesses vastly expanded frontal, temporal, and posterior parietal cortices

(Elston et al., 2006; Kaas, 2012) that share dense reciprocal connectivity with the primate ACC, implying that the ACC is involved in a broad range of computations, which these areas perform (Roberts and Clarke, 2019). Interpreting comparative work in species that lack the complex cortical structures that are connected to the ACC make it difficult to translate conclusions about the psychological role the ACC plays across respective species. That is, if psychological functions emerge from complex brain networks, then similar brain regions that sit within different networks are likely to have different psychological functions. It is therefore critical to study the ACC using a nonhuman primate model to better understand the causal role this structure, and the networks to which it belongs, play in supporting complex psychological phenomena.

The ACC appears to be consistently, and in some cases critically, involved in linking computations of affective value to behavioral outputs (for review, see Heilbronner and Hayden, 2016). For example, ACC activity is consistently observed when animals need to generate behavior based on the value, including changing value, of stimuli—particularly those related to reward (Amiez et al., 2006; Baeg et al., 2009; Amemori and Graybiel, 2012), punishment (Amemori and Graybiel, 2012), when information about behavioral errors are present (Niki and Watanabe, 1976; Ito et al., 2003), and when contextual information potentially modulates the affective value of stimuli and actions (Baeg et al., 2009). Despite consistent ACC activity during the processing and updating of reward information (Amiez et al., 2006; Kennerley et al., 2009; Kennerley and Wallis, 2009), some evidence from monkeys with ACC damage suggests that they are able to update the representations of reward value that are linked to an object and an action based on current biological context (Chudasama et al., 2013; but see Hadland et al., 2003b), pointing to the possible dissociation between ACC functions identified via electrophysiological studies and those identified via lesion/deactivation studies.

In that vein, damage to, or causally manipulating activity of, the nonhuman primate ACC modulates the generation of affect-related behaviors, although the pattern of effects is not particularly clear and is likely related to variations in methodology and the area targeted. For example, when affect-related overt behavioral responses have been evaluated relative to threat, as in these experiments, monkeys with ACC sulcus (area 24) damage were faster to retrieve a food item placed near a moving snake than control animals. In the same experiment, however, ACC gyrus (areas 24 and 32) damage did not have the same effect and when tested with a nonmoving (rubber) snake, animals with both ACC sulcus lesions or the ACC gyrus lesions behaved like controls with regard to their food retrieval behavior (Rudebeck et al., 2006). Animals with ACC gyrus lesions also generated fewer overt behaviors in the presence of robust valued social stimuli (videos of other monkeys), although when only ostensibly positive behaviors were considered, both ACC gyrus-lesioned animals and ACC sulcus-lesioned animals generated fewer behaviors than control animals (Rudebeck et al., 2006). Compared with controls, monkeys with complete ACC lesions manipulated neutral objects more and generated fewer affect-related vocalizations in social contexts (Hadland et al., 2003a). Further, microstimulation of a subpopulation of neurons within area 25 of rhesus monkeys has been shown to increase avoidance behavior toward an aversive stimulus (Amemori and Graybiel, 2012), and pharmacological inactivation of area 25 increased baseline heart rate variability, and decreased cardiac reactivity to threat in marmosets (Wallis et al., 2017). In contrast, pharmacological inactivation of area 32 enhanced cardiac and behavioral reactivity toward threat (Wallis et al., 2017). However, local valence-related heterogeneity is observed within cytoarchitectonic regions (e.g., neurons in area 25 are sensitive to both positive and negative stimuli as in the study by Amemori and Graybiel, 2012), complicating matters further. These findings, in concert with ours, all coalesce around the idea that the ACC is involved in threat processing, although previous literature points to the ACC being involved in variations in the magnitude of behavioral responses to threat while our data point to the ACC being involved in sustaining the magnitude over time. One reason for this difference may be that previous lesion studies, including those above that tested animals with objects (Hadland et al., 2003a; Rudebeck et al., 2006), used aspiration lesions that almost certainly did some damage to the white matter underlying the ACC, which itself could have altered affective behavior (for review, see Bubb et al., 2018). In contrast, our neurotoxic lesions largely spared fibers of passage by design and therefore may better illustrate the role of the ACC per se in affective reactivity.

Although ACC lesions did not change the overall magnitude of affective responses, they did attenuate maintenance of reactivity over time. Neurologically intact control animals sustained their reactivity over test days, but the reactivity of ACC-lesioned animals decreased over test days in both experiments. Of note, the human intruder task presented the same exact stimulus (same person engaging in the same behavior) over 5 test days, and thus one possible interpretation is that monkeys with ACC lesions habituated to the repeated presentations differently than controls. In contrast, however, the object responsiveness task presented different stimuli on each test day, and so habituation to specific stimuli is not a likely explanation for the effects. Instead, the data are consistent with a pattern of findings present in the human imaging and nonhuman primate lesion and recording literatures, which suggests that the ACC may be critical for maintaining or sustaining affective and attentional responding in appropriate contextually dependent ways, including over different time scales (Kennerley et al., 2006; Rudebeck et al., 2014; Carl et al., 2016). Evidence that speaks to this sort of effect is on a notably shorter time scale than the current experiment. For example, monkeys with damage to the subgenual ACC (area 25) are unable to normally sustain their autonomic arousal between the presentations of cues that predict reward and the delivery of reward within a given trial (timescale, 2.5 s; Rudebeck et al., 2014). Similarly, monkeys with damage to the both banks of ACC sulcus of area 24 were unable to sustain reward-related behavioral responses across trials within a test session; they were seemingly able to use error-related information to correct behavior but unable to use positive reinforcement information to maintain correct responding over time (Kennerley et al., 2006). That is, there is now evidence that damage to different regions of the ACC perturbs sustenance of affective responding over seconds (Rudebeck et al., 2014), minutes (Kennerley et al., 2006), and also days (the present report), although these studies (like other lesion studies of the ACC and recording studies of the ACC) target different anatomic subregions. This failure to sustain appropriate affective responding over a time course of days, rather than seconds, is consistent with the purported role of the ACC in depression (for review, see Drevets et al., 2008; Mulders et al., 2015), for which a core feature is reduced affective responding across long time courses (American Psychiatric Association, 2013).

Our work here is part of a larger conversation about the neurobiology of threat processing and anxiety, which has been

extensively investigated in behavioral neuroscience using the two threat-responding tasks we used in this report: the human intruder task and the object responsiveness task. Decades of research using similar tasks have suggested that the amygdala plays a putative role in affective processing by modulating the magnitude of responses to threats that can be indexed with tasks like these, although the magnitude and pattern of effects vary more than might be expected across specific study and both across and within laboratory groups (for discussion, see Charbonneau et al., 2021b). In general, the amygdala is thought to be important for modulating the magnitude of threat on the basis that some studies have found that amygdala damage dramatically reduces negative affect-related behaviors (aggression, submission, stress/anxiety/tension-related behaviors, and/or defensiveness) and/or increases the likelihood of approaching and/or interacting with potentially threatening stimuli (Aggleton and Passingham, 1981; Meunier et al., 1999; Stefanacci et al., 2003; Kalin et al., 2004; Mason et al., 2006; Machado and Bachevalier, 2008). In some cases, similar effects related to sustaining responding across time were documented following amygdala damage (e.g., there were only lesion group differences in the first 3 d of testing on human intruder but not subsequent test days, (Mason et al., 2006) or no remarkable lesion group differences at all (Kalin et al., 2001; Izquierdo et al., 2005; Charbonneau et al., 2021b). Studies of other parts of the brain have yielded similarly mixed results. For example, similar experiments have demonstrated that animals with orbitofrontal cortex (OFC) damage have reduced reactivity during human intruder (less freezing than controls; Kalin et al., 2007; Fox et al., 2010), although other studies have demonstrated that they have heightened "mild aggression" compared with controls (Izquierdo et al., 2005). OFC damage seems to cause reduced affective reactivity during object responsiveness (faster interactions with snakes; Izquierdo et al., 2005; Kalin et al., 2007) and reduced defensive behavior and increased approach behavior compared with controls (Izquierdo et al., 2005), although damage to similar areas of marmoset OFC causes increases in anxious behavior (Agustín-Pavón et al., 2012). The variability across studies, even those conducted in the same laboratory using the same protocols (Charbonneau et al., 2021b; Mason et al., 2006), has largely been ignored as being important but may be related to variations in experimental conditions, such as social housing conditions (Charbonneau et al., 2021a), lesion methodology (for discussion, see Meunier et al., 1999), or even the timing of experiments relative to surgery. Further, variability also likely reflects the fact that affective reactivity is not a modular behavioral function but is realized by multiple distributed neural networks that compute affective value and organize behavioral responses to it, and thus damage to one focal area may be compensated for by other hubs in the network.

In closing, focal and complete damage to the ACC impacts the vigor and vigilance of affective responding to threats over time and repeated presentations, but not the overall magnitude of response to threat, at least initially. The preservation of both the initial reactivity to ostensible threat and appropriately scaling the threat response is likely because of the presence of other intact neural regions responsible for initial detection and behavioral response to threat/novelty (e.g., anterior insula, amygdala). Our findings are consistent with recent suggestions that the ACC is particularly important for processing aspects of threat (Roberts, 2020), and the observation that the ability to sustain threat responding over time and repeated occurrences of threats, as the neurologically intact control animals did, is mediated in part by the ACC. The extent to which the ACC is necessary for sustaining normative behavioral responding over time or contextual shifts in other contexts (e.g., during social interactions) remains an open question to be evaluated in future work.

References

Aggleton JP, Passingham RE (1981) Syndrome produced by lesions of the amygdala in monkeys (Macaca mulatta). J Comp Physiol Psychol 95:961–977.

Agustín-Pavón C, Braesicke K, Shiba Y, Santangelo AM, Mikheenko Y, Cockroft G, Asma F, Clarke H, Man M-S, Roberts AC (2012) Lesions of ventrolateral prefrontal or anterior orbitofrontal cortex in primates heighten negative emotion. Biol Psychiatry 72:266–272.

Alexander L, Wood CM, Gaskin PLR, Sawiak SJ, Fryer TD, Hong YT, McIver L, Clarke HF, Roberts AC (2020) Over-activation of primate subgenual cingulate cortex enhances the cardiovascular, behavioral and neural responses to threat. Nat Commun 11:5386.

Amemori K, Graybiel AM (2012) Localized microstimulation of primate pregenual cingulate cortex induces negative decision-making. Nat Neurosci 15:776–785.

American Psychiatric Association (2013) Diagnostic and statistical manual of mental disorders (DSM-5). Arlington, VA: American Psychiatric Publishing.

Amiez C, Joseph J-P, Procyk E (2006) Reward encoding in the monkey anterior cingulate cortex. Cereb Cortex 16:1040–1055.

Baeg EH, Jackson ME, Jedema HP, Bradberry CW (2009) Orbitofrontal and anterior cingulate cortex neurons selectively process cocaine-associated environmental cues in the rhesus monkey. J Neurosci 29:11619–11627.

Barbas H, Pandya D (1989) Architecture and intrinsic connections of the prefrontal cortex in the rhesus monkey. J Comp Neurol 286:353–375.

Bartra O, McGuire JT, Kable JW (2013) The valuation system: a coordinate-based meta-analysis of BOLD fMRI experiments examining neural correlates of subjective value. Neuroimage 76:412–427.

Bates D, Mächler M, Bolker B, Walker S (2014) Fitting linear mixed-effects models using lme4. arXiv: 1406.5823v1.

Bliss-Moreau E, Baxter MG (2018) Estradiol treatment in a nonhuman primate model of menopause preserves affective reactivity. Behav Neurosci 132:224–229.

Bliss-Moreau E, Moadab G (2016) Variation in behavioral reactivity is associated with cooperative restraint training efficiency. J Am Assoc Lab Anim Sci 55:41–49.

Bliss-Moreau E, Toscano JE, Bauman MD, Mason WA, Amaral DG (2010) Neonatal amygdala or hippocampus lesions influence responsiveness to objects. Dev Psychobiol 52:487–503.

Bliss-Moreau E, Toscano JE, Bauman MD, Mason WA, Amaral DG (2011) Neonatal amygdala lesions alter responsiveness to objects in juvenile macaques. Neuroscience 178:123–132.

Bubb EJ, Metzler-Baddeley C, Aggleton JP (2018) The cingulum bundle: anatomy, function, and dysfunction. Neurosci Biobehav Rev 92:104–127.

Bush G, Luu P, Posner MI (2000) Cognitive and emotional influences in anterior cingulate cortex. Trends Cogn Sci 4:215–222.

Capitanio JP (1999) Personality dimensions in adult male rhesus macaques: Prediction of behaviors across time and situation. American Journal of Primatology 47:299–320.

Capitanio JP, Mendoza SP, Cole SW (2011) Nervous temperament in infant monkeys is associated with reduced sensitivity of leukocytes to cortisol's influence on trafficking. Brain Behav Immun 25:151–159.

Carl H, Walsh E, Eisenlohr-Moul T, Minkel J, Crowther A, Moore T, Gibbs D, Petty C, Bizzell J, Dichter GS, Smoski MJ (2016) Sustained anterior cingulate cortex activation during reward processing predicts response to psychotherapy in major depressive disorder. J Affect Disord 203:204–212.

Charbonneau JA, Amaral DG, Bliss-Moreau E (2021a) Social housing status impacts rhesus monkeys' affective responding in classic threat processing tasks. bioRxiv. 2021.05.16.444352.

Charbonneau JA, Bennett JL, Bliss-Moreau E (2021b) Amygdala or hippocampus damage only minimally impacts affective responding to threat. Behav Neurosci, in press.

Chudasama Y, Daniels TE, Gorrin DP, Rhodes SE, Rudebeck PH, Murray EA (2013) The role of the anterior cingulate cortex in choices based on reward value and reward contingency. Cereb Cortex 23:2884–2898.

Delignette-Muller ML, Dutang C (2015) fitdistrplus: an R package for fitting distributions. J Stat Soft 64:1–34.
Drevets WC, Savitz J, Trimble M (2008) The subgenual anterior cingulate cortex in mood disorders. CNS Spectr 13:663–681.
Dum RP, Strick PL (2002) Motor areas in the frontal lobe of the primate. Physiol Behav 77:677–682.
Ebitz RB, Hayden BY (2016) Dorsal anterior cingulate: a Rorschach test for cognitive neuroscience. Nat Neurosci 19:1278–1279.
Elston GN, Benavides-Piccione R, Elston A, Zietsch B, Defelipe J, Manger P, Casagrande V, Kaas JH (2006) Specializations of the granular prefrontal cortex of primates: implications for cognitive processing. Anat Rec A Discov Mol Cell Evol Biol 288:26–35.
Enel P, Wallis JD, Rich EL (2020) Stable and dynamic representations of value in the prefrontal cortex. Elife 9:e54313.
Fox AS, Shelton SE, Oakes TR, Converse AK, Davidson RJ, Kalin NH (2010) Orbitofrontal cortex lesions alter anxiety-related activity in the primate bed nucleus of stria terminalis. J Neurosci 30:7023–7027.
Fox AS, Oler JA, Birn RM, Shackman AJ, Alexander AL, Kalin NH (2018) Functional connectivity within the primate extended amygdala is heritable and associated with early-life anxious temperament. J Neurosci 38:7611–7621.
Fox J, Weisberg S (2019) An R companion to applied regression, Ed 3. Thousand Oaks, CA: Sage.
Glees P, Cole J, Whitty C, Cairns H (1950) The effects of lesions in the cingular gyrus and adjacent areas in monkeys. J Neurol Neurosurg Psychiatry 13:178–190.
Gottlieb DH, Capitanio JP (2013) Latent variables affecting behavioral response to the human intruder test in infant rhesus macaques (Macaca mulatta): latent variables in rhesus intruder test. Am J Primatol 75:314–323.
Grayson DS, Bliss-Moreau E, Bennett J, Lavenex P, Amaral DG (2017) Neural Reorganization Due to Neonatal Amygdala Lesions in the Rhesus Monkey: Changes in Morphology and Network Structure. Cerebral Cortex 27:3240–3253.
Hadland KA, Rushworth MFS, Gaffan D, Passingham RE (2003a) The effect of cingulate lesions on social behaviour and emotion. Neuropsychologia 41:919–931.
Hadland KA, Rushworth MFS, Gaffan D, Passingham RE (2003b) The anterior cingulate and reward-guided selection of actions. J Neurophysiol 89:1161–1164.
Hamel AF, Lutz CK, Coleman K, Worlein JM, Peterson EJ, Rosenberg KL, Novak MA, Meyer JS (2017) Responses to the human intruder test are related to hair cortisol phenotype and sex in rhesus macaques (Macaca mulatta). Am J Primatol 79:1–10.
Hartig F (2020) DHARMa: residual diagnostics for hierarchical (multi-level/mixed) regression models. Vienna, Austria: R Project for Statistical Computing.
Heilbronner SR, Hayden BY (2016) Dorsal anterior cingulate cortex: a bottom-up view. Annu Rev Neurosci 39:149–170.
Isomura Y, Ito Y, Nambu A, Takada M (2003) Neural Coding of "Attention for Action" and "Response Selection" in Primate Anterior Cingulate Cortex. J Neurosci 23:8002–8012.
Ito S, Stuphorn V, Brown JW, Schall JD (2003) Performance monitoring by the anterior cingulate cortex during saccade countermanding. Science 302:120–122.
Izquierdo A, Murray EA (2004) Combined unilateral lesions of the amygdala and orbital prefrontal cortex impair affective processing in rhesus monkeys. J Neurophysiol 91:2023–2039.
Izquierdo A, Suda R, Murray E (2005) Comparison of the effects of bilateral orbital prefrontal cortex lesions and amygdala lesions on emotional responses in rhesus monkeys. J Neurosci 25:8534–8542.
Kaas JH (2012) The evolution of neocortex in primates. Prog Brain Res 195:91–102.
Kalin N, Shelton SE (1989) Defensive behaviors in infant rhesus monkeys: environmental cues and neurochemical regulation. Science 243:1718–1721.
Kalin NH, Shelton SE (1998) Ontogeny and stability of separation and threat-induced defensive behaviors in rhesus monkeys during the first year of life. Am J Primatol 44:125–135.
Kalin NH, Shelton SE, Davidson RJ, Kelley AE (2001) The primate amygdala mediates acute fear but not the behavioral and physiological components of anxious temperament. J Neurosci 21:2067–2074.
Kalin NH, Shelton SE, Davidson RJ (2004) The role of the central nucleus of the amygdala in mediating fear and anxiety in the primate. J Neurosci 24:5506–5515.
Kalin NH, Shelton SE, Davidson RJ (2007) Role of the primate orbitofrontal cortex in mediating anxious temperament. Biol Psychiatry 62:1134–1139.
Kennerley SW, Wallis JD (2009) Encoding of reward and space during a working memory task in the orbitofrontal cortex and anterior cingulate sulcus. J Neurophysiol 102:3352–3364.
Kennerley SW, Walton ME, Behrens TEJ, Buckley MJ, Rushworth MFS (2006) Optimal decision making and the anterior cingulate cortex. Nat Neurosci 9:940–947.
Kennerley SW, Dahmubed AF, Lara AH, Wallis JD (2009) Neurons in the frontal lobe encode the value of multiple decision variables. J Cogn Neurosci 21:1162–1178.
Laubach M, Amarante LM, Swanson K, White SR (2018) What, if anything, is rodent prefrontal cortex? Eneuro 5:ENEURO.0315-18.2018.
Lavenex P, Lavenex PB, Bennett JL, Amaral DG (2009) Postmortem changes in the neuroanatomical characteristics of the primate brain: hippocampal formation. J Comp Neurol 512:27–51.
Lenth R (2020) emmeans: estimated marginal means, aka least-squares means. Vienna, Austria: R Project for Statistical Computing.
Lindquist KA, Wager TD, Kober H, Bliss-Moreau E, Barrett LF (2012) The brain basis of emotion: a meta-analytic review. Behav Brain Sci 35:121–143.
Machado CJ, Bachevalier J (2008) Behavioral and hormonal reactivity to threat: effects of selective amygdala, hippocampal or orbital frontal lesions in monkeys. Psychoneuroendocrinology 33:926–941.
Mantini D, Gerits A, Nelissen K, Durand J-B, Joly O, Simone L, Sawamura H, Wardak C, Orban GA, Buckner RL, Vanduffel W (2011) Default mode of brain function in monkeys. Journal of Neuroscience 31:12954–12962.
Mason WA, Capitanio JP, Machado CJ, Mendoza SP, Amaral DG (2006) Amygdalectomy and responsiveness to novelty in rhesus monkeys (macaca mulatta): generality and individual consistency of effects. Emotion 6:73–81.
Meunier M, Bachevalier J, Mishkin M (1997) Effects of orbital frontal and anterior cingulate lesions on object and spatial memory in rhesus monkeys. Neuropsychologia 35:999–1015.
Meunier M, Bachevalier J, Murray EA, Málková L, Mishkin M (1999) Effects of aspiration versus neurotoxic lesions of the amygdala on emotional responses in monkeys. Eur J Neurosci 11:4403–4418.
Mirsky AF, Rosvold HE, Pribram KH (1957) Effects of cingulectomy on social behavior in monkeys. J Neurophysiol 20:588–601.
Mulders PC, van Eijndhoven PF, Schene AH, Beckmann CF, Tendolkar I (2015) Resting-state functional connectivity in major depressive disorder: a review. Neurosci Biobehav Rev 56:330–344.
Murray E, Davidson M, Gaffan D, Olton D, Suomi S (1989) Effects of fornix transection and cingulate cortical ablation on spatial memory in rhesus monkeys. Exp Brain Res 74:173–186.
Niki H, Watanabe M (1976) Cingulate unit activity and delayed response. Brain Res 110:381–386.
Pandya DN, Van Hoesen GW, Mesulam MM (1981) Efferent connections of the cingulate gyrus in the rhesus monkey. Exp Brain Res 42:319–330.
Parker A, Gaffan D (1997) The effect of anterior thalamic and cingulate cortex lesions on object-in-place memory in monkeys. Neuropsychologia 35:1093–1102.
Perry A, Roberts G, Mitchell PB, Breakspear M (2019) Connectomics of bipolar disorder: a critical review, and evidence for dynamic instabilities within interoceptive networks. Mol Psychiatry 24:1296–1318.
Prather M, Lavenex P, Mauldin-Jourdain M, Mason W, Capitanio J, Mendoza S, Amaral DG (2001) Increased social fear and decreased fear of objects in monkeys with neonatal amygdala lesions. Neuroscience 106:653–658.
Pribram KH, Fulton JF (1954) An experimental critique of the effects of anterior cingulate ablations in monkey. Brain 77:34–44.
R Core Team (2019) R: a language and environment for statistical computing. Vienna, Austria: R Project for Statistical Computing.
Roberts AC (2020) Prefrontal regulation of threat-elicited behaviors: a pathway to translation. Annu Rev Psychol 71:357–387.
Roberts AC, Clarke HF (2019) Why we need nonhuman primates to study the role of ventromedial prefrontal cortex in the regulation of threat- and reward-elicited responses. Proc Natl Acad Sci U S A 116:26297–26304.

Rolls ET (2019) The cingulate cortex and limbic systems for emotion, action, and memory. Brain Struct Funct 224:3001–3018.
Rudebeck PH, Buckley MJ, Walton ME, Rushworth MF (2006) A role for the macaque anterior cingulate gyrus in social valuation. Science 313:1310–1312.
Rudebeck PH, Putnam PT, Daniels TE, Yang T, Mitz AR, Rhodes SE, Murray EA (2014) A role for primate subgenual cingulate cortex in sustaining autonomic arousal. Proc Natl Acad Sci U S A 111:5391–5396.
Rudebeck PH, Rich EL, Mayberg HS (2019) From bed to bench side: reverse translation to optimize neuromodulation for mood disorders. Proc Natl Acad Sci U S A 116:26288–26296.
Rushworth M, Hadland K, Gaffan D, Passingham R (2003) The effect of cingulate cortex lesions on task switching and working memory. J Cogn Neurosci 15:338–353.
Rushworth M, Walton ME, Kennerley SW, Bannerman D (2004) Action sets and decisions in the medial frontal cortex. Trends Cogn Sci 8:410–417.
Rushworth M, Behrens T, Rudebeck P, Walton M (2007) Contrasting roles for cingulate and orbitofrontal cortex in decisions and social behaviour. Trends Cogn Sci 11:168–176.
Seeley WW (2019) The salience network: a neural system for perceiving and responding to homeostatic demands. J Neurosci 39:9878–9882.
Smith W (1944) The results of ablation of the cingular region of the cerebral cortex. Fed Proc 3:42.
Stefanacci L, Amaral DG (2002) Some observations on cortical inputs to the macaque monkey amygdala: an anterograde tracing study. J Comp Neurol 451:301–323.
Stefanacci L, Clark RE, Zola SM (2003) Selective neurotoxic amygdala lesions in monkeys disrupt reactivity to food and object stimuli and have limited effects on memory. Behav Neurosci 117:1029–1043.
Therneau TM (2020) coxme: mixed effects Cox models. Vienna, Austria: R Project for Statistical Computing.
Touroutoglou A, Bliss-Moreau E, Zhang J, Mantini D, Vanduffel W, Dickerson BC, Barrett LF (2016) A ventral salience network in the macaque brain. NeuroImage 132:190–197.
Vincent JL, Patel GH, Fox MD, Snyder AZ, Baker JT, Van Essen DC, Zempel JM, Snyder LH, Corbetta M, Raichle ME (2007) Intrinsic functional architecture in the anaesthetized monkey brain. Nature 447:83–86.
Vogt BA (2009) Regions and subregions of the cingulate cortex. In: Cingulate neurobiology and disease, pp 3–30. Oxford, UK: Oxford UP.
Vogt BA, Paxinos G (2014) Cytoarchitecture of mouse and rat cingulate cortex with human homologies. Brain Struct Funct 219:185–192.
Vogt BA, Vogt L, Farber NB, Bush G (2005) Architecture and neurocytology of monkey cingulate gyrus. J Comp Neurol 485:218–239.
Vogt BA, Hof PR, Zilles K, Vogt LJ, Herold C, Palomero-Gallagher N (2013) Cingulate area 32 homologies in mouse, rat, macaque and human: cytoarchitecture and receptor architecture. J Comp Neurol 521:4189–4204.
Wallis CU, Cardinal RN, Alexander L, Roberts AC, Clarke HF (2017) Opposing roles of primate areas 25 and 32 and their putative rodent homologs in the regulation of negative emotion. Proc Natl Acad Sci U S A 114:E4075–E4084.